FEATURES OF THE CRYSTAL STRUCTURE OF ZnO:Mn NANOCRYSTALS OBTAINED BY ULTRASONIC SPRAY PYROLYSIS

O.V. Kovalenko*, V.Yu. Vorovsky, V.O. Makarov, Ye.G. Plakhtii

Oles Honchar Dnipro National University, Dnipro, Ukraine
**e-mail: kovalenko.dnu@gmail.com*

Samples of ZnO and ZnO:Mn nanocrystals with Mn 2 and 4 at.% impurity concentrations obtained by ultrasonic spray pyrolysis were studied by X-ray diffraction. It was determined that the reflexes of the X-ray diffractions of the samples had a shift relative to the standard position towards large diffraction angles. This indicated the nonequilibrium state of the crystal lattice, which caused the appearance of strain stresses. Debye–Scherrer and Williamson–Hall methods were used to calculate the parameters of the crystal lattice, the size of nanocrystals, and strain stresses with different concentrations of Mn. When the concentration of Mn increased to 4 at.%, there was an increase in strain stresses in nanocrystals by 10 times in comparison with undoped ZnO. The unit cell volume of ZnO:Mn nanocrystals was significantly smaller in comparison with single-crystal ZnO, which indicated that they had their intrinsic defects.

Keywords: zinc oxide, ZnO:Mn nanocrystals, crystal lattice, strain stress, intrinsic defects.

Received 08.11.2021; Received in revised form 09.12.2021; Accepted 10.12.2021

1. Introduction

Nanocrystalline (NC) ZnO is widely used in solar cells, gas sensors, ultraviolet light emitters, transparent electrodes, etc. Recently, interest in this material has increased significantly because when it is doped with transition metals, it reveals ferromagnetic properties at room temperature [1]. Diluted magnetic semiconductors (DMS), which include ZnO nanocrystals (NCs) doped with manganese, are of considerable interest due to the possibility of constructing spintron devices for storing and recording information on their basis [2].

Among the known methods of synthesis of DMS, the method of ultrasonic spray pyrolysis (USP) differs favorably from all other ones because it is non-vacuum and easy for implementation. It allows obtaining nanomaterials both in the form of powder and films [3]. This method is based on the thermal decomposition of aerosol droplets of the initial solution during their passage through the thermal zone. In this case, the thermal decomposition takes place in the atmosphere of the carrier gas and the final product is released on a screen filter heated to the appropriate temperature. It is possible to control such parameters of the final product as the size of NCs and surface defects in this method. It also allows to alloy NCs with various impurities [4]. When USP method is used, the obtained NCs can be surrounded by an amorphous intercrystalline environment, which affects the state of the crystal lattice [5]. The physical properties of semiconducting materials are determined by their band structure and crystal lattice parameters. Therefore, much attention is paid to the study of the crystal structure of DMS obtained by various methods. The works [6, 7] carried out the study of strain stresses ε of the crystal lattice of ZnO NCs obtained at low temperatures of synthesis. It is shown that the parameters of the crystal lattice and the volume of the unit cell decrease in the NCs. This leads to the appearance of crystal lattice strain stresses.

The authors believe that the cause of this phenomenon may be the appearance of NC defects – vacancies of oxygen and zinc. A study of the effect of Mn impurity concentration on strain stresses in ZnO:Mn NCs was performed in [8]. The analysis of X-ray diffraction by the Williamson-Hall method showed that increasing the Mn impurity concentration to 8 at.% leads to an increase of ε 60 times. ZnO NCs obtained by the electrolytic method were studied in [9]. According to the approximation line of the analysis results of X-ray diffraction by the Williamson–Hall method, it was found that stresses act in ZnO NC, which affect the shift of reflexes and the half-width. The obtained value ε in ZnO NC equals $9.6 \cdot 10^{-4}$. The samples of ZnO NCs obtained by sedimentaion method in a polyethylene glycol solution were studied in

[10]. The effect of deformation stresses on the broadening of the peaks of X-ray diffraction was estimated using the Williamson-Hall formula. The value ε in ZnO NC, which equals $15.6 \cdot 10^{-4}$, was obtained as a result of calculations. The value $\varepsilon = 19.8 \cdot 10^{-4}$ in ZnO:Mn NC with Mn concentration of 10 at.% synthesized by the sol-gel method was obtained in [11].

Analysis of the literature indicates that the structural parameters and deformation stresses ε in ZnO and ZnO:Mn NCs largely depend on the synthesis conditions. Equilibrium synthesis conditions lead to the formation of a stable crystal lattice with parameters a and c close to the parameters of single-crystal ZnO and a small value of ε. As is well known, the synthesis of ZnO:Mn NCs occurs at nonequilibrium conditions by using USP method. In this case, NCs are formed with a defective structure of the "core – shell" type – a defect-free core and a defective shell, and NC can be surrounded by an amorphous intercrystalline environment [4]. Such conditions of the formation of NCs lead to significant changes in the parameters of the crystal lattice, as well as the appearance of deformation stresses in it. Therefore, the aim of this work is to study the influence of the doping process of ZnO NC with Mn impurity on the deformation stress of the crystal lattice.

2. Synthesis method and calculation of crystal lattice parameters

We studied ZnO:Mn NC samples with a manganese concentration of 2 and 4 at.% obtained by USP method. The precursors in the synthesis were zinc nitrates ($Zn(NO_3)_2 \cdot 6H_2O$) and manganese nitrates $Mn(NO_3)_2 \cdot 6H_2O$. A prepared 10% aqueous solution of zinc nitrate with the required amount of manganese nitrate was sprayed onto aerosol droplets with $d = 1 \div 2$ μm size. These droplets were transported with the help of a carrier gas (air) through the heated reaction zone of the furnace, where the droplets were dried and the ZnO:Mn NCs were synthesized for a limited time (7 ÷ 10 sec). The synthesized product in the form of spherical granules was accumulated on the filter at a temperature of 250 ºC. The synthesis of the samples was carried out at a temperature of T = 550 ºC.

The study of the crystal structure and phase composition of the samples was carried out by X-ray diffraction (XRD) at a DRON-2M diffractometer using Co K_α (λ = 1,7902 Å) emission. The unit cell parameters a and c were calculated from the position of individual reflexes after repeated scanning of the diffraction peak profiles with an accuracy of 0.01 degrees.

The calculations of the crystal structure parameters were carried out in the following sequence. Initially, the position of the reflexes on the XRD of the samples was analyzed to determine the type of crystal structure. These positions correspond to the Wolf–Bragg equation:

$$2d_{hkl} \sin(\theta) = n\lambda \qquad (1)$$

where d_{hkl} is the spacing between planes of given Miller indices h, k, and l, is the angle between the incident beam and the reflection plane, n is a positive whole number (order of reflection), λ is the X-ray wavelength.

The obtained X-ray diffraction of the samples were used to calculate the values of the average NC size, crystal lattice parameters and unit cell volume. The average size of the ZnO:Mn NC was calculated using the Debye–Scherrer formula [12]:

$$D = \frac{k\lambda}{\beta \cos\theta} \qquad (2)$$

where k = 0.9, λ is the X-ray wavelength (λ = 1.7902 Å), β is the total angular width of the reflex at half the maximum of the peaks, θ is the angle between the incident beam and the reflection plane.

The values of the lattice parameters a and c for the samples were determined by the equalities:

$$a = \frac{\lambda}{2sin\theta}\sqrt{\frac{4}{3}\left(h^2\alpha + hk + k^2\right) + \frac{l^2}{(c/a)^2}} \quad (3)$$

$$c = \frac{\lambda}{2sin\theta}\sqrt{\frac{4}{3(a/c)^2}(h^2 + hk + k^2) + l^2)} \quad (4)$$

So, the lattice constant a for the reflex (100) was calculated by the formula

$$a = \frac{\lambda}{\sqrt{3}\,sin\theta}, \quad (5)$$

the lattice constant c for the reflex (002) was calculated by the formula

$$c = \frac{\lambda}{sin\theta} \quad (6)$$

and the unit cell volume for the hexagonal structure was calculated using the expression

$$V = \frac{\sqrt{3}a^2c}{2} = 0{,}866a^2c\,. \quad (7)$$

It is possible to use the Debye–Scherrer formula (2) if there are no deformation stresses in the crystal lattice. In this case, the total angular width of the reflex β is determined only by the NC size. Such conditions are fulfilled in NC samples obtained at high synthesis temperatures or after prolonged (for many hours) thermal treatments. The angular broadening of the reflex β under other synthesis conditions is defined as

$$\beta = \beta_S + \beta_D \quad (8)$$

where β_S is the integral line width due only to the size effect and is the integral line width due to the presence of deformation stresses.

Differentiating the Wolf–Bragg equation (1) and taking into account formula (2), it is possible to obtain the relation for

$$\beta_D = 4 \cdot tg\,\theta \quad (9)$$

Thus, in the presence of deformation stresses, the expansion increases in direct proportion to $tg\theta$. In their absence, in accordance with (2), the expansion increases inversely to $cos\theta$.

Williamson and Hall [13] proposed a graphical method for determining the NC size and the magnitude of deformation stresses using a plot of β versus $sin\theta$ and $cos\theta$ in the

assumption that the size and strain contribution functions are described by Lorentz functions. Therefore, equation (8), taking into account (2) and (9), has the form:

$$\beta \cdot \cos\theta = \frac{0.9\lambda}{D} + 4\varepsilon \cdot \sin\theta \tag{10}$$

Equation (10) is the straight-line equation with the argument If a straight line is drawn through a series of experimental values , the inclination angle will be proportional to the ε value, and the intersection of the graph with the *y* axis allows calculating the average size *D*.

The calculation of the structural parameters, such as the parameters of the crystal lattice *a* and *c*, the volume of the unit cell *V* was carried out according to formulas (5) – (7). The deformation stresses of the NC crystal lattice were determined on the basis of equation (10). In this case, the integral line width at half maximum of the reflex is calculated for reflexes (100), (002), (101), (102), (110), (103).

3. Results and discussion

The X-ray diffraction patterns of ZnO and ZnO:Mn NC samples synthesized by USP method at the temperature of 550 °C with Mn concentration 2 and 4 at.% were subject to analysis. The X-ray diffraction of the samples (Fig. 1, a) showed no reflexes of impurity phases. This indicated that single phase connections had been obtained. The crystal structure of ZnO:Mn NC was a hexagonal wurtzite type (according to the standard JCPDS card: 36-1451). An increase in the Mn concentration led to a decrease in the crystallinity of the samples – the intensity of the reflexes decreased; the lines became broader.

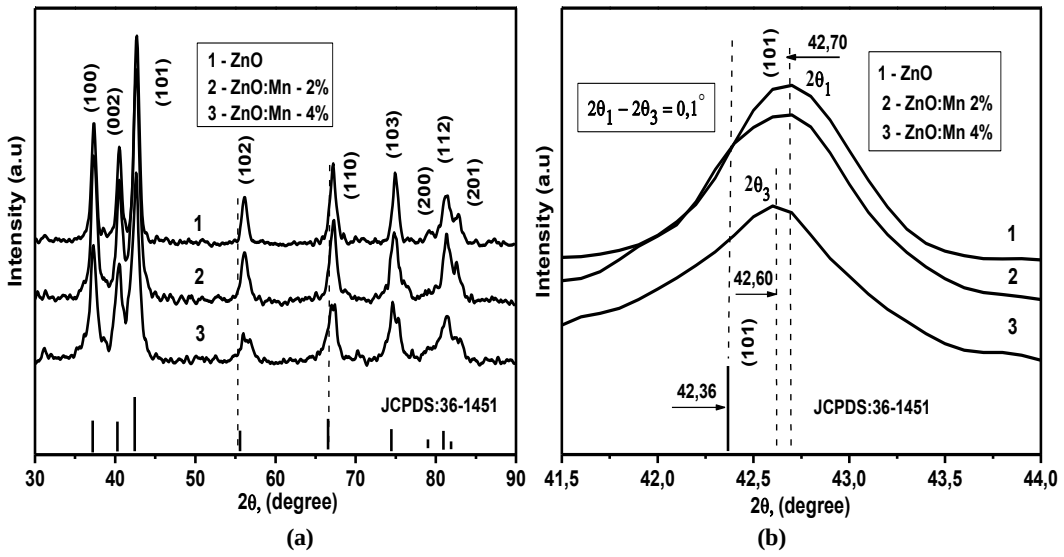

Fig. 1: a – X-ray diffractions patterns of synthesized samples at the temperature of *T* = 550 °C; b – shift of reflex (101): 1 – a sample of ZnO, 2 – ZnO: Mn-2at%, 3 - ZnO:Mn-4at%.

The analysis of the obtained X-ray diffraction patterns showed that the positions of the reflexes were shifted with respect to the standard values for ZnO towards large diffraction angles. It can be seen from the analysis of reflexes (101) (Fig. 1, b) that the displacement of the reflexes on X-ray diffraction patterns of ZnO sample relative to the standard ($2\theta_{101}$ = 42.36°) has a value $\Delta(2\theta)$ = 0.34°. Such shift of reflections, taking into

account the Wolf–Bragg formula (1), indicates a decrease in the interplanar distances *d*, which causes the appearance of deformation stresses in the crystal lattice of NCs. Thus, the synthesis of ZnO:Mn NC is characterized by a nonequilibrium state of their crystal lattice. A shift in the positions of reflexes with an increase in the Mn concentration relative to the synthesized sample of ZnO NC towards small diffraction angles is also observed. The shift reaches the value $\Delta(2\theta) = 0.1°$ for ZnO:Mn NC sample with the manganese concentration of 4 at.%. This shift is explained by the partial doping of the samples with manganese, since the ionic radius of Mn^{2+} (0.83 Å) is larger than ionic radius of Zn^{2+} (0.74 Å) [4].

The calculation of the structural parameters using formulas (2) – (7) shows that the volume of a unit cell *V* increases when ZnO is doped with manganese (Table 1). In this case, there is a substitution of Zn^{2+} ions at the nodes of the crystal lattice by Mn^{2+} ions, which have a larger ionic radius. The average NC size calculated using the Debye–Scherrer formula ($D_{D–S}$) decreases with Mn concentration increasing. This tendency is characteristic for the process of NC growth from solution, since when an impurity atom hits the crystalline surface of NC, the rate of its growth in this direction decreases. Values of the average size of NC obtained by the Williamson–Hall method ($D_{W–H}$) grow with Mn concentration increasing. This is due to an increase in the deformation stresses of the crystal lattice of NC when ZnO is doped with a Mn impurity and the presence of an additional broadening of the reflection lines in (8).

Table 1

Structural parameters of samples ZnO, ZnO:Mn-2at.% and ZnO:Mn-4at.%.

Samples	*hkl*	2θ°	β°	*a*, Å	*c*, Å	*V*, Å^3	*D*, нм (D–S)	*D*, нм (W–H)	ε, $\times 10^{-4}$
ZnO	100	37.366	0.859	3.2307	-	46.753	10.3	11.9	5.9
	002	40.499	0.933	-	5.1725		9.6		
ZnO:Mn 2 at.%	100	37.346	0.730	3.2317	-	46.780	10.3	12.9	17.5
	002	40.505	0.714	-	5.1718		9.6		
ZnO:Mn 4 at.%	100	37.270	0.914	3.2386		46.985	9.7	14.5	51.9
	002	40.495	1.050		5.1728		8.5		

Calculations of the deformation stresses of the crystal lattice of NC according to equation (10) for reflexes (100), (002), (101), (102), (110), (103) show that the experimental values of the dependence of on are approximated by linear functions (Fig. 2):

$$Y_1 = 0.01256 + 0.00059X \text{ – for ZnO sample;}$$

$$Y_2 = 0.01341 + 0.00176X \text{ – for ZnO:Mn-2 at.\% sample;} \quad (11)$$

$$Y_3 = 0.01106 + 0.00519X \text{ – for ZnO:Mn-4 at.\% sample.}$$

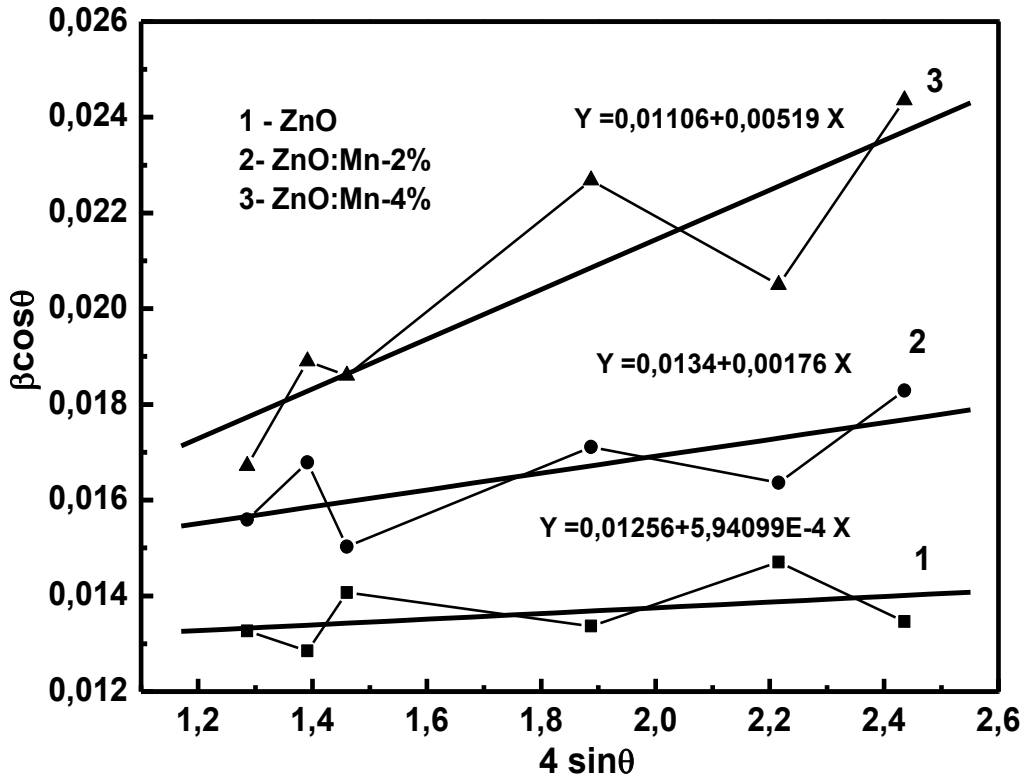

Fig. 2. Results of the analysis of samples by the Williamson–Hall method: 1 – ZnO sample, 2 – ZnO:Mn-2at.% sample, 3 – ZnO:Mn-4at.% sample.

The angular coefficients of the approximating straight lines are positive (Fig. 2), which indicates the action of tensile stresses in the NCs. The presence of this type of deformation stresses was also detected in ZnO NC synthesized by the electrolytic method [9]. The existence of such deformation stresses is confirmed by the established fact of the shift of reflexes towards large diffraction angles (Table 1), which corresponds to a decrease in the interplanar spacings *d* in the crystal lattice of NC relative to their equilibrium values in single-crystal ZnO. The obtained values of deformation stresses ε (Table 1) indicate that they increase when ZnO is doped with manganese. The unit cell volume *V* of ZnO:Mn NC samples has a much lower value compared to single-crystal ZnO, for which $V = 47.589$ Å^3 [14]. This indicates the disordering of the crystal lattice of the samples synthesized by USP method and, according to the authors' conclusions of the papers [6, 7], also the presence of a significant number of intrinsic defects, namely oxygen vacancies (V_o) and intergranular zinc (Zn_i). The volume of the unit cell of ZnO:Mn NC tends to decrease upon doping; therefore, it can be concluded that Mn impurity activates the formation of oxygen vacancies in ZnO:Mn NC.

4. Conclusions

It was found that the reflexes of the X-ray diffraction patterns were shifted with respect to the standard values for ZnO towards large diffraction angles in ZnO:Mn NC. This indicates that the crystal lattice is in a nonequilibrium state and has deformation stresses. The obtained parameters of the crystal cell *a* and *c*, as well as the volume of the unit cell *V* are significantly lower than those of single-crystal ZnO. It is assumed that this is a consequence of the presence of a significant number of intrinsic defects in the NC. Calculations of NC sizes and deformation stresses in the crystal lattice of ZnO:Mn NC have been carried out.

The analysis of X-ray diffraction of the samples by the Williamson–Hall method showed that an increase in Mn concentration led to an increase in the deformation stresses of the crystal lattice of NC by 10 times in comparison with undoped ZnO. It is shown that an increase in deformation stresses in ZnO:Mn NC can be associated with an increase in the concentration of defects (oxygen vacancies V_o). Thus, the main feature of the crystal structure of ZnO:Mn NC obtained by USP method is the disordered deformation stress state of the crystal lattice in the presence of a large number of intrinsic defects.

References

1. **Sharma, P.** Ferromagnetism above room temperature in bulk and transparent thin films of Mn-doped ZnO / P. Sharma, A. Gupta, K. Rao [et al.] // Nature Materials. – 2003. – Vol. 2, No. 10. – P. 673 – 677.

2**. Pogorily, S. M.** Spintronics. Basic Phenomena. Trends of Development / S. M. Pogorily, S. M. Ryabchenko, A. I. Tovstolitkin// Ukr. J. Phys. Review – 2010. – Vol. 6. – P. 37 – 97.

3. **Tsai, S. C.** Ultrasonic spray pyrolysis for nanoparticles synthesis / S. C. Tsai, Y. L. Song, C. S. Tsai, C. C. Yang, at al.// Journal of Materials Science. – 2004. – Vol. 39, No.11. – P. 3647 – 3657.

4. **Vorovsky, V. Yu.** Preparation of zinc oxide nanopowders doped with manganese which have ferromagnetic properties at room temperature / V. Yu. Vorovsky, A. V. Kovalenko, A. I. Kushneryov, O. V. Khmelenko // Functional Materials. – 2018. – Vol.25, No.1. – P. 1 – 6.

5. **Gleiter, H.** Materials with ultrafine microstructures: retrospectives and perspectives / H. Gleiter // Nanostructured Materials. – 1992. – Vol. 1, No.1. – P. 1 – 19.

6. **Kalita, A.** Size dependence of lattice parameters in ZnO nanocrystals / A. Kalita, M. P. C. Kalita // Applied Physics A. – 2015. – Vol. 121, No. 2. – P. 521 – 524.

7. **Zeng, H.** Blue luminescence of ZnO nanoparticles based on non-equilibrium processes: defect origins and emission controls / H. Zeng, G. Duan, Y. Li, S. Yang, X. Xu, W. Cai // Advanced Functional Materials. – 2010. – Vol. 20, No. 4. – P. 561 – 572.

8. **Sharma, P. K.** Doping, strain, defects and magneto-optical properties of $Zn_{1-x}Mn_xO$ nanocrystals / P. K. Sharma, R. K. Dutta, R. J. Choudhary, A. C. Pandey // Cryst. Eng. Comm. – 2013. – Vol. 15, No. 22. – P. 4438 – 4447.

9. **Danilevskaya, N. B.** Fabrication and Properties of Nanostructured ZnO and ZnS / N. B. Danilevskaya, N. V. Moroz, B. D. Nechyporuk, B. P. Rudyk // Journal of Nano- and Electronic Physics. – 2016. – Vol. 8, No. 1. – P. 01006-01010.

10. **Yogamalar, R.** X-ray peak broadening analysis in ZnO nanoparticles / R. Yogamalar, R. Srinivasan, A. Vinu, K. Ariga, A. C. Bose // Solid State Communications. – 2009. – Vol. 149, No. 43-44. – P. 1919 – 1923.

11. **Yoon, D. H.** Synthesis, structural, and magnetic properties of Co-doped and Mn-doped ZnO nanocrystalline DMS prepared by the facile polyvinyl alcohol gel method / D.

H. Yoon, K. Raju // Journal of Superconductivity and Novel Magnetism. – 2017. – Vol. 30, No. 1. – P. 203 – 208.

12. **Patterson, A. L.** The Scherrer Formula for X-Ray Particle Size Determination / A. L. Patterson // Physical Review. – 1939. – Vol. 56, No. 10. – P. 978 – 981.

13. **Williamson, G. K.** X-ray line broadening from filed aluminium and wolfram/ G. K. Williamson, W. H. Hall // Acta Metallurgica. – 1953. – Vol. 1. – No. 1. – P. 22 – 31.

14. **Özgür, Ü.** Comprehensive review of ZnO materials and devices / Ü. Özgür, Y. I. Alivov, C. Liu, A. Teke, M. Reshchikov [et al.] // Journal of Applied Physics. – 2005. – Vol. 98(4). – P. 041301-103.